Data dependent weights in discontinuous weighted least-squares approximation with anisotropic support

Calcolo

ISSN 0008-0624
Volume 48
Number 1

Calcolo (2010) 48:127-143
DOI 10.1007/
s10092-010-0032-7

Springer

Calcolo (2011) 48: 127–143
DOI 10.1007/s10092-010-0032-7

Data dependent weights in discontinuous weighted least-squares approximation with anisotropic support

N.B. Petrovskaya

Received: 17 November 2009 / Accepted: 9 July 2010 / Published online: 23 September 2010

Abstract Discontinuous weighted least-squares (DWLS) approximation is modification of a weighted least-squares method that requires a local support (a reconstruction stencil) to approximate a function at a given point. A DWLS method is often employed in computational problems where a function is approximated on an irregular computational grid. It has recently been revealed that the method provides inaccurate approximation on irregular grids and conventional weighting of distant points captured by a reconstruction stencil on an irregular coarse mesh does not improve the accuracy of the approximation. Thus in our paper we further investigate the impact of distant points on the accuracy of DWLS approximation and design new weight coefficients for DWLS reconstruction that allow one to obtain more accurate reconstruction results. Our approach is based on a concept of numerically distant points originally developed in author's previous works, as a new weight function calculates the distance between two points in the data space.

Keywords Weighted least-squares approximation · Coarse mesh · Directional error estimates

Mathematics Subject Classification (2000) 65D05 · 65Z05 · 68U10

1 Introduction

A least-squares (LS) method is one of the most well known approaches in solving a problem of finding the best polynomial approximation to the input data [12]. While

This paper is part of a special issue devoted to the 2nd Dolomites Workshop on Constructive Approximation and Applications, 2009.

N.B. Petrovskaya (✉)
School of Mathematics, University of Birmingham, Edgbaston, Birmingham B15 2TT, UK
e-mail: n.b.petrovskaya@bham.ac.uk

general accuracy estimates of the LS method are based on the assumption that all observations made to get LS data should provide equally precise information, data used in many practical applications are of varying quality in terms of the uncertainty of the measurement. Thus a widespread approach is to use weighted least-squares (WLS) approximation to improve the accuracy of LS approximation. In a WLS method weight coefficients are allocated to least-squares data in order to suppress data points where the observation error can be large [6, 12]. As a large error of LS approximation is often associated with distant points in the data set, many authors recommend to choose a weight of each data point as a function of the inverse distance between two given points (e.g., see [1, 2, 5, 10, 23]).

Discontinuous weighted least-squares (DWLS) approximation is modification of a WLS method that approximates a given function at each point belonging to a set of points selected over a computational grid. A DWLS reconstruction is very similar to a moving least-squares (MLS) method [9], as the coefficients of the approximation depend on the location of a point where the reconstruction is made. The MLS approximation has successfully been adapted in meshless methods used as an alternative to finite element methods in solution of various heat transfer and fluid flow problems (e.g., see [18]), while the DWLS reconstruction is currently used in higher-order finite volume schemes heavily exploited in computational aerodynamics [3, 4, 10]. However, the difference between a DWLS and an MLS procedure is that in the latter case a local support for the approximation is prescribed by the definition of a weight function in the problem, while for the DWLS approximation a local support (also called a reconstruction stencil) is entirely determined by the edge data structure on a computational grid. The weight function in a DWLS method is only used to improve the accuracy of the approximation on a given stencil by reducing the measurement error, as it has been mentioned above.

One basic feature of DWLS reconstruction that stems from the nature of computational problems where the method is exploited is that a reconstruction stencil may present a highly irregular geometry. The DWLS reconstruction on irregular meshes remains a challenging and difficult problem as the method can lose accuracy to unacceptable limit [10, 16, 20, 22]. A general problem of weighted least-squares approximation with irregular (anisotropic) support has received little attention in the literature so far (cf. discussion in [7, 15]). A research effort in meshless methods that use MLS approximation was mainly focused on the shape of weight functions to mitigate the impact of an irregular point distribution in the problem. Meanwhile, the optimal radius of the support cannot be implemented in a DWLS problem, as the size of a reconstruction stencil is prescribed by a geometry of a computational mesh.

Earlier insight into the problem attributed poor accuracy of the method on irregular grids to the impact of distant points on the results of DWLS reconstruction. However, it recently turned out that inverse distance weighting of stencil points is not always efficient in practical computations [16, 20]. A detailed discussion of a DWLS method with highly irregular support has been provided in recent papers [16, 17] where a concept of numerically distant points has been introduced. While geometrically distant points are remote points in the physical space, numerically distant points are defined as distant points in the data space. In practical applications numerically distant points appear in reconstruction stencils on irregular coarse meshes that are usually generated at the initial stage of a solution grid adaptation procedure. Such points are a result of poor solution resolution as a numerical solution on coarse meshes is an essentially discrete function whose properties can be significantly different from its continuous counterpart.

It has been shown in [16] that numerically distant points in reconstruction stencil seriously affect the accuracy of DWLS approximation. Meanwhile, standard methods such as inverse distance weighting in a geometric domain cannot eliminate numerically distant points from a reconstruction stencil, as those points can be located close to the origin $P_0 = (x_0, y_0)$ where the DWLS reconstruction should be computed. Other techniques are required in order to provide more accurate reconstruction on irregular coarse meshes where the accuracy control is a challenging task as asymptotic error estimates cannot be applied on such meshes. Thus in the present paper we design new weight coefficients to deal with numerically distant points in a reconstruction stencil. The new weights depend on a function to be approximated by a DWLS method and are different from the weights in the physical space. Using data dependent weights in a DWLS reconstruction problem allows one to detect numerically distant points and to efficiently eliminate them from the stencil. Our approach is illustrated by numerical examples.

2 The discontinuous weighted least-squares reconstruction

In this section we explain the formulation of a DWLS method along with the definition of a local reconstruction stencil used for the approximation. Consider a two-dimensional domain Ω and a set of points $P_i = (x_i, y_i) \in \Omega$, $i = 1, \dots, N$. Weighted least-squares (WLS) approximation deals with data $\mathbf{U}$ at points P_i, where $U_i = U(P_i)$ can be considered as the value of a continuous function $U(x, y)$ at a given point P_i. The data $\mathbf{U}$ should be fitted to the function

$$u(x, y) = \sum_{k=0}^{M} u_k \phi_k(x, y), \quad M < N, \tag{1}$$

where $\mathbf{u} = (u_0, u_1, u_2, \dots, u_M)$ are fitting parameters, and $\phi_k(x, y)$, $k = 0, \dots, M$, are polynomial basis functions. The unknown parameters $\{u_k\}$ are determined in the WLS method by seeking the minimum of the following merit function (*e.g.*, see [12, 19]),

$$F_w^2 = \sum_{i=1}^{N} w(\bar{P}, P_i) \left[U(P_i) - u(P_i)\right]^2, \tag{2}$$

where the weight function $w(\bar{P}, P)$ is defined for a fixed point $\bar{P} \in \Omega$. Taking partial derivatives with respect to the fitting parameters u_k, $k = 0, \dots, M$, to find out $\min_{\mathbf{u}} F^2$, we obtain $M + 1$ normal equations of the WLS problem

$$\sum_{i=1}^{N} w(\bar{P}, P_i) \left[U_i - \sum_{j=0}^{M} u_j \phi_j(P_i) \right] \phi_k(P_i) = 0, \quad k = 0, \dots, M.$$

The normal equations can be written in the matrix form as

$$\mathbf{A}^T\mathbf{A}\mathbf{u} = \mathbf{A}^T\mathbf{U}, \tag{3}$$

where the design matrix $\mathbf{A}$ is as follows

$$A_{ij} = \phi_j(P_i), \quad i = 1, \ldots, N, \ j = 0, \ldots, M,$$

the matrix $\mathbf{A}_{wls} = \mathbf{A}^T\mathbf{W}\mathbf{A}$, the vector $\mathbf{b}_{wls} = \mathbf{A}^T\mathbf{W}\mathbf{U}$ and a diagonal weight matrix $\mathbf{W}$ is defined as

$$W_{ij} = \begin{cases} w(\bar{P}, P_i), & i = j, \\ 0, & \text{otherwise}; \ i, j = 1, 2, \ldots, N. \end{cases}$$

Equations (3) are solved for the vector $\mathbf{u}$,

$$\mathbf{u} = \mathbf{A}_{wls}^{-1}\mathbf{b}_{wls}, \tag{4}$$

to obtain the WLS approximation at point $\bar{P}$.

The choice of the weight function $w(\bar{P}, P_i)$ depends on a given problem under consideration. In many approximation problems the weight function $w(\bar{P}, P)$ is defined to mitigate the impact of distant points on the accuracy of the approximation. For this purpose the weight function is chosen as a function of Euclidean distance $r = \|\bar{P} - P_i\|$ between point $\bar{P}$ and a given point P_i. In MLS problems, where the weight function is required to provide a compact support for the least-squares approximation, the Gaussian or the spline weight function is the most popular choice [11, 13, 15], but other weight functions can also be found in the literature [1, 23].

An important feature of the WLS approximation is that the solution $\mathbf{u}$ becomes a function of $\bar{P}$, and the fitting parameters $\{u_k\}$ have to be recomputed for any new $\bar{P}$. The global approximation in this case can be achieved by imposing additional conditions on the approximation, such as the requirement that the supports of the weight functions entirely cover the domain Ω. On the contrary, discontinuous weighted least-squares (DWLS) approximation remains local approximation, and no additional conditions are required to reconstruct the function (1) in the domain of interest. Below we introduce the DWLS approximation on an arbitrary computational grid.

Let an unstructured computational grid G with grid nodes $P_i = (x_i, y_i)$, $i = 1, 2, \ldots, N_G$, be generated in the domain Ω (see Fig. 1 where a fragment of a triangular unstructured grid is shown) and the global data vector $\mathbf{U}_G = (U_1, U_2, \ldots, U_{N_G})$ be defined at nodes of grid G. Consider a discrete set of points $\bar{P}_l$, $l = 1, \ldots, L$, over the grid G, where the data $\mathbf{U}_G$ should be approximated at each $\bar{P}_l$. The definition of the set $\{\bar{P}_l\}$ is based on a given computational problem. In finite volume discretization schemes, where DWLS approximation is intensively exploited, the set $\{\bar{P}_l\}$ is often considered as a set of all edge midpoints taken on the grid G. For the definition of DWLS approximation at point $\bar{P}_l$ a local support S_l (a reconstruction stencil) is allocated for each point $\bar{P}_l$ as follows. The two nodes n_1 and n_2 that comprise the edge e_l are identified, and S_l consists of all nodes that belong to edges incident to the node n_1 or n_2. Thus the support S_l appears as a subset of N grid nodes, $S_l \subset G$, chosen

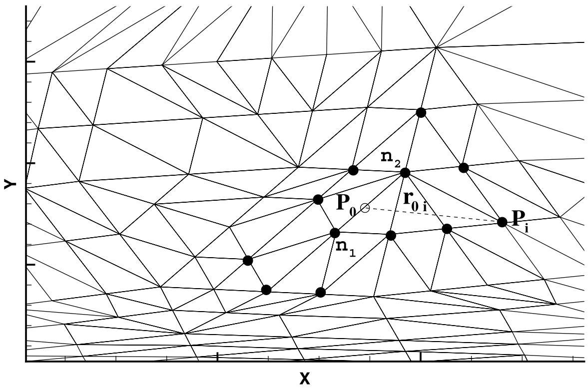

Fig. 1 An example of a reconstruction stencil for DWLS approximation on an irregular grid. Stencil members for the reconstruction at point P_0 are shown as *black circles*

by a known rule for local WLS approximation at point $\bar{P}_l$. Once the reconstruction stencil S_l has been allocated, local numbering is used in the approximation problem. Namely, the point $\bar{P}_l$ is denoted as P_0, and the support points are numbered as P_i, $i = 1, \ldots, N$. An example of the reconstruction stencil on an irregular unstructured grid is shown in Fig. 1.

The next step in the definition of the DWLS approximation is to allocate a local data vector $\mathbf{U} = (U_1, U_2, \ldots, U_N)$ by taking the entries of $\mathbf{U}_G$ at stencil points. The WLS approximation is then implemented to reconstruct the solution at point P_0. The weight function conventionally exploited in DWLS problems is

$$w(P_0, P_i) \equiv w(r_{0i}) = r_{0i}^{-p}, \quad p = 0, 1, 2, \ldots, \tag{5}$$

where p is an integer polynomial degree and $r_{0i} = \sqrt{(x_0 - x_i)^2 + (y_0 - y_i)^2}$ is the distance between the point P_i, $i = 1, 2, \ldots, N$, of the stencil and the point P_0 (see Fig. 1). The weights of stencil points are controlled by polynomial degree p. The unweighted reconstruction corresponds to $p = 0$, while $p > 0$ provides inverse distance weighting used to mitigate the impact of remote stencil points on the results of DWLS approximation.

Once the function has been reconstructed at the point $P_0 \equiv \bar{P}_l$, the next point $\bar{P}_{l+1}$ is taken and the reconstruction procedure is repeated. Thus the fit functions $\{\phi_k\}$ remain discontinuous in Ω, as the DWLS approximation is computed at each point $\bar{P}_l$ independently. However, we should mention here that DWLS approximation does not require a user to assemble global approximation over the domain Ω, as the formulation of problems, where the DWLS reconstruction is used, implies that we are interested in the approximation at each point P_l considered separately (e.g., see [16] for details). That allows one to consider a DWLS method as truly local approximation where the computational cost of the algorithm is relatively low. It is the local nature of the DWLS approximation that makes the method attractive for projection-evolution schemes exploited in modern computational aerodynamics [3, 10, 20], as using DWLS in a higher order finite volume scheme makes it possible to increase the order of the scheme without increasing the total number of degrees of freedom.

One essential feature of DWLS reconstruction is that the local support S_l may present a highly irregular geometry. The accuracy of DWLS reconstruction with an irregular support remains the main concern in practical applications, as a DWLS method degrades to unacceptable accuracy on irregular coarse meshes that should be considered at the initial stage of a solution grid adaptation procedure. Consequently, poor accuracy of DWLS reconstruction used in a projection-evolution scheme affects the convergence of a numerical solution by generating large discretization errors and ill-conditioned matrices. In recent years the intensive study of factors that may make an impact on the accuracy of the approximation has been performed for computational aerodynamics problems [10, 16, 17, 20, 22], as the DWLS reconstruction problem remains crucial for the progress in design and implementation of modern industrial codes. However, while the impact of grid geometry was in the focus of the recent research, little attention has been paid to the properties of a function that should be reconstructed on an irregular coarse mesh. The first attempt to take those properties into account has been made in the work [17], where the concept of numerically distant points has been introduced. Furthermore, it has been shown in [16, 17] that numerically distant points can even be more dangerous for the accuracy of DWLS reconstruction than geometrically distant points. Thus for the rest of the paper we discuss how to handle numerically distant points that appear in DWLS reconstruction on irregular meshes.

3 The accuracy of DWLS approximation on irregular meshes: numerically distant points

In this section we first briefly remind the idea of conventional weighting in the physical space used to eliminate geometrically distant points from a reconstruction stencil. We then explain the concept of numerically distant points and demonstrate that inverse distant weighting does not work when the stencil contains numerically distant points.

The problem of geometrically distant points can be illustrated by a simple example of a harmonic function discussed below. Let us notice that the Laplace equation is often considered to be a good model for investigating a discretization of the diffusion operator in the Navier-Stokes equations. Thus a finite volume discretization of the Laplace equation, where DWLS reconstruction of the solution gradient is an essential discretization requirement, has intensively been studied and validated in various computational aerodynamics problems.

Consider the following solution to Laplace's equation

$$U(x) = \frac{1}{2}((x-A)^2 - (y-A)^2), \tag{6}$$

where the parameter A is taken as $A = 10.0$ in our computations. Let the set of stencil points be defined as

$$P_i = (R\cos\phi_i, R\sin\phi_i), \tag{7}$$

where $\phi_i = \frac{\pi}{4}(2i-1),\ i = 1, \ldots, 4$ and the radius $R = 0.1$ (see Fig. 2). Let us now add a remote point $P_5 = (10.0, 7.0)$ to the stencil and look at the results of DWLS reconstruction at the origin $P_0 = (0, 0)$.

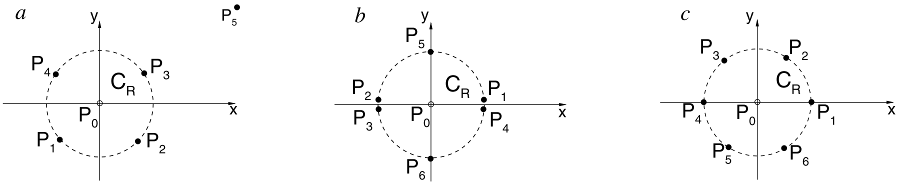

Fig. 2 Reconstruction stencil geometries for the DWLS test cases. (**a**) A reconstruction stencil includes a geometrically distant point P_5. (**b**) A reconstruction stencil includes numerically distant points P_5 and P_6 that are not geometrically distant points. (**c**) All stencil points are equidistant, but weights in the solution space are not the same as weights in the physical space

We consider linear DWLS approximation at the point P_0,

$$u_{DWLS}(x, y) = \sum_{k=0}^{2} u_k \phi_k(x, y), \tag{8}$$

where $\phi_k(x, y) = (x - x_0)^\alpha (y - y_0)^\beta,\ \alpha + \beta = 0, 1$. We are interested in the reconstruction error,

$$e(P_0) = |U(P_0) - u_{DWLS}(P_0)|, \tag{9}$$

and the gradient error,

$$e_\nabla(P_0) = \|\nabla U(x, y) - \nabla u_{DWLS}(x, y)\|_{|P_0}, \tag{10}$$

at the origin P_0, where the gradient vector is $\nabla = (\partial/\partial x, \partial/\partial y)$ and the norm $\|\nabla g(x, y)\|$ is defined as $\sqrt{(\frac{\partial g(x,y)}{\partial x})^2 + (\frac{\partial g(x,y)}{\partial y})^2}$. The errors are first computed for unweighted reconstruction, where we take $p = 0$ in the function (5). The function error and the gradient error are $e(P_0) = 2.4148\text{e–}02$, $e_\nabla(P_0) = 1.78745$, respectively. The large gradient error can be attributed to the presence of a distant point P_5 in the reconstruction stencil (see Fig. 2a) and we expect that data weighting will mitigate the impact of a distant point on the accuracy of the reconstruction.

The results of the implementation of the weight function (5) in the DWLS reconstruction (8) are shown in Table 1. The function error (9) and the gradient error (10) are shown in the table for various polynomial degrees p in (5). It can be seen from the table that the weighting of stencil points reduces the error of the DWLS reconstruction, as a remote point P_5 becomes effectively eliminated from the stencil by assigning a very small weight to it.

The above example justifies inverse distance weighting in computations on anisotropic meshes, and many authors recommend weighting (5) in a DWLS problem in order to suppress distant points in a reconstruction stencil and to obtain accurate approximation [4, 10, 22]. Meanwhile, it recently turned out that implementation of the weight function (5) still provides very inaccurate results on irregular coarse grids. Several examples illustrating the accuracy of a DWLS method on computational grids used in industrial applications that require numerical solution of the Navier-Stokes equations have been discussed in papers [16, 17, 20, 22].

Table 1 Inverse distance weighting of geometrically distant points. The function error $e(P_0)$ and the gradient error $e_\nabla(P_0)$ are computed for DWLS reconstruction (8) of the function (6). The error (9) and (10) are obtained for various polynomial degrees p in the weight function (5)

p	0	1	2	3	4
$e(P_0)$	8.5563e–04	8.4188e–04	2.8523e–04	3.4908e–06	2.8714e–08
$e_\nabla(P_0)$	2.08869	2.05631	6.96314e–01	8.52214e–02	7.00997e–05

In recent paper [17] a novel idea of numerically distant points in a reconstruction stencil has been introduced and such points have been defined as stencil points that are distant points in the data space. While recognition of geometrically distant points is a straightforward task, it is difficult to detect numerically distant points in the stencil, as their definition depends essentially on a function $U(x, y)$ under consideration. Such points can be close to the origin $P_0 = (x_0, y_0)$, where the function $U(x, y)$ is reconstructed, but the function value measured at a numerically distant point still has a big data error that affects the accuracy of DWLS reconstruction. As numerically distant points are not remote points in a geometric domain, weighting (5) cannot eliminate them from a reconstruction stencil.

One example of numerically distant points in a reconstruction stencil is given by the following function

$$U(x, y) = 2x^2 + \exp(2By). \tag{11}$$

Let us design a reconstruction stencil for the function (11) that does not contain any geometrically distant points. Namely, we require that $x_i^2 + y_i^2 = R^2$ for any stencil point P_i, $i = 1, \dots, 6$. The stencil points are then located at the circle C_R as follows (see Fig. 2b),

$$\begin{aligned} P_i &= ((-1)^{i+1} R\cos\alpha, R\sin\alpha), \quad i = 1, 2, \\ P_i &= ((-1)^{i} R\cos\alpha, -R\sin\alpha), \quad i = 3, 4, \\ P_i &= (0, (-1)^{i+1} R), \quad i = 5, 6. \end{aligned} \tag{12}$$

As in the previous test case, we compute the function error (9) and the gradient error (10) at the origin $P_0 = (0, 0)$. Let parameter $B = 3$, the radius $R = 0.8$ and the angle $\alpha = \frac{\pi}{16}$, then the function error and the gradient error for the unweighted reconstruction are $e(P_0) = 21.0549$ and $e_\nabla(P_0) = 65.0566$, respectively.

It is obvious that the implementation of the weight function (5) in the problem will result in the same error values, as the weights are given by $w(r_{0i}) = 1/R^p = const$ for all stencil points by the definition of the reconstruction stencil. Meanwhile, if we eliminate points P_5 and P_6 from the stencil, we will get an essentially smaller error, $e(P_0) = 1.70273$, $e_\nabla(P_0) = 9.16169\text{e–}01$, over a new stencil $S_l = \{P_1, P_2, P_3, P_4\}$ (see Fig. 2b). Hence, the points P_5 and P_6, which are not geometrically distant stencil points, can be considered as numerically distant points in the problem, as including them into the stencil worsen the accuracy of DWLS approximation.

An important observation about the DWLS support is that points P_5 and P_6 are not numerically distant points in reconstruction stencil (12) if the function (6) is considered. The error computation for the DWLS reconstruction of the function (6) over stencil (12) gives us $e(P_0) = 9.04276\text{e–}02$, $e_\nabla(P_0) = 1.28095\text{e–}14$. At the same time, the error is $e(P_0) = 2.95641\text{e–}01$, $e_\nabla(P_0) = 5.37623\text{e–}14$, if we consider stencil $S = \{P_1, P_2, P_3, P_4\}$ for the DWLS reconstruction of (6) at point P_0.

The test case above shows that the definition of a numerically distant point in the stencil depend on a given function $U(x, y)$. In other words, a point $P_i = (x_i, y_i)$, considered as a numerically distant point for approximation of $U(x, y)$, would belong to a correct range of observations if another function $\tilde{U}(x, y)$ were considered. Ideally a weight function should mitigate the impact of numerically distant points defined by the function $U(x, y)$ as well as it mitigates the impact of geometrically distant points on the accuracy of the DWLS reconstruction. Thus in the next section we design an approach that allows one to measure the distance between points in the data space rather than in the physical space.

To conclude this section, let us emphasize it again that we discuss the DWLS error on a given grid rather than the convergence rate of the method. Obviously, careful grid refinement (that is decreasing the maximum radius in the test cases above) would result in a smaller error of the DWLS approximation. However, we are interested in the error reduction on a given grid with fixed geometry as in many practical applications a large reconstruction error on an irregular coarse grid makes further grid refinement impossible.

4 Data dependent weights in DWLS approximation

Consider the merit function for unweighted LS approximation,

$$F^2 = \sum_{i=1}^{N} [U(P_i) - u(P_i)]^2 . \tag{13}$$

Our aim is to re-formulate the LS problem defined by the function (13) in terms of the minimization of the interpolation error. Let us denote by Π_1 the set of all real linear polynomials $\pi(x, y)$,

$$\pi(x, y) = \sum_{k=0}^{2} a_k \psi_k(x, y), \tag{14}$$

where $\psi_k(x, y) = x^\alpha y^\beta,\ \alpha + \beta = 0, 1$. The following theorem (e.g., see [21]) states the uniqueness of the linear interpolation.

Theorem 1 *Consider three arbitrary support points* $(\hat{P}_i, U(\hat{P}_i))$, $i = 1, 2, 3$ *for linear interpolation of the function* $U(x, y)$ *by polynomial* $\pi(x, y)$, *where we require that* $\hat{P}_i \neq \hat{P}_{i'}$ *for* $i \neq i'$. *Then there exists a unique polynomial* $\pi(x, y) \in \Pi_1$ *with* $\pi(\hat{P}_i) = U(\hat{P}_i)$, $i = 1, 2, 3$.

Consider linear DWLS approximation (8). Once coefficients u_k in the expansion (8) have been defined, the expansion (8) can be thought of as linear interpolation of the function $U(x, y)$. In other words, it follows from Theorem 1 that there exist three points, $\hat{P}_1$, $\hat{P}_2$ and $\hat{P}_3$, such that the following condition holds

$$\sum_{k=0}^{2} u_k \phi_k(\hat{P}_l) = U(\hat{P}_l), \quad l = 1, 2, 3.$$

Let us denote the linear polynomial defined by (8) as $\hat{\pi}(x, y)$. The function (13) can then be rewritten as

$$F^2 = \sum_{i=1}^{N} \left[U(P_i) - \hat{\pi}(P_i)\right]^2 = \sum_{i=1}^{N} E_i^2, \tag{15}$$

where $E_i = |U(P_i) - \hat{\pi}(P_i)|$ is the interpolation error taken at point P_i. Hence the minimization of the merit function is equivalent to the minimization of the interpolation error at all stencil points, and we conclude that those stencil points where the interpolation error is large should be eliminated from the stencil by means of weighting.

It is obvious that we do not know the interpolation error as the expansion coefficients $\{u_k\}$ in (8) are not known to us when we define weights in the reconstruction problem. However, we can use interpolation error estimates in a DWLS problem. Let us connect points P_0 and P_i in order to define edge e_i of the reconstruction stencil, where the edge length is $r_{0i}^2 = (x_i - x_0)^2 + (y_i - y_0)^2$ (see Fig. 1). Consider a function $U(x, y) \in C^2$ and let $\pi(x, y)$ be a linear interpolant (14) of $U(x, y)$. The interpolation error E_i at the edge e_i is then given by (*e.g.*, see [8, 14])

$$E_i = |U(x, y) - \pi(x, y)| = r_{0i}^2 \left| \frac{\partial^2 U(\xi_i)}{\partial \tau_i^2} \right|,$$

where τ_i is the unit tangential vector and point $\xi_i \in e_i$. The error E_i can be rewritten as

$$E_i = |r_{0i}^T \mathbf{H} r_{0i}| = r_{0i}^T |\mathbf{H}| r_{0i},$$

where the Hessian matrix $\mathbf{H}$ is defined at point ξ_i as

$$H_{kl} = \frac{\partial^2 U}{\partial x_k \partial x_l}, \quad k = 1, 2, \ l = 1, 2,$$

and the notation $(x, y) \equiv (x_1, x_2)$ is used for points in the physical space.

We now replace the directional derivative at unknown point ξ_i by its value at point $P_{i+1/2} = (\frac{1}{2}(x_0 + x_i), \frac{1}{2}(y_0 + y_i))$ in order to obtain the interpolation error estimate at the edge e_i,

$$E_i = r_{0i}^2 \left| \frac{\partial^2 U(P_{i+1/2})}{\partial \tau_i^2} \right| = r_{0i}^T |\mathbf{H}|_{P_{i+1/2}} r_{0i}, \tag{16}$$

where the Hessian is now computed at the edge midpoint $P_{i+1/2}$.

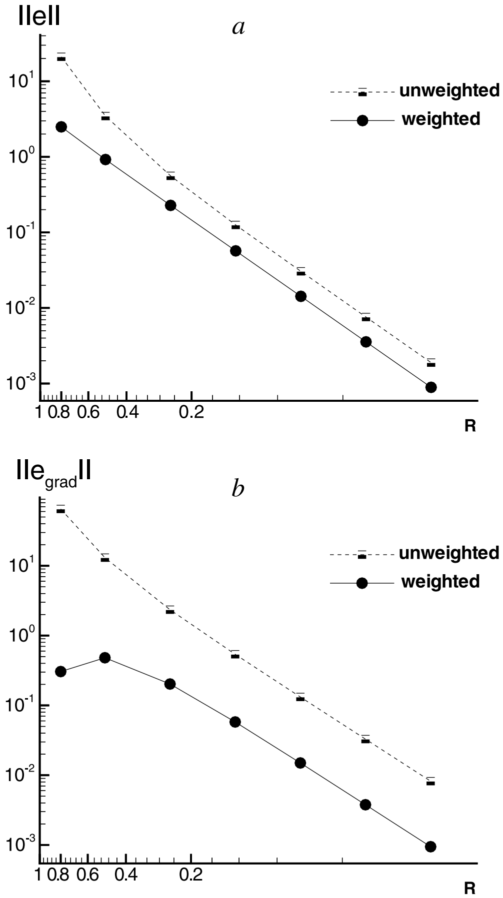

Fig. 3 The convergence rate for linear DWLS approximation of the function (11). The weight function (18) is used to eliminate numerically distant points from the stencil. (**a**) The function error (9) for the weighted (*solid line*) and unweighted (*dashed line*) approximation. (**b**) The gradient error (10) for the weighted (*solid line*) and unweighted (*dashed line*) approximation

The matrix $\mathbf{H}$ in (16) can be decomposed as $\mathbf{H} = \mathbf{R}\boldsymbol{\Lambda}\mathbf{R}^{-1}$, where $\boldsymbol{\Lambda}$ is a diagonal matrix of the eigenvalues of $\mathbf{H}$, $\mathbf{R}$ is the matrix of right eigenvectors of $\mathbf{H}$, and the matrix $\mathbf{R}^{-1} = \mathbf{R}^T$. Hence we can introduce the metric tensor $\mathcal{M}$ at point $P_{i+1/2}$ as $\mathcal{M} = \mathbf{R}|\boldsymbol{\Lambda}|\mathbf{R}^{-1}$. The transformation defined by the metric tensor $\mathcal{M}$ is a rotation mapping of the R^2 canonical basis onto the unit eigenvectors of $\mathbf{H}$. Then the error estimate (16) gives us the edge length $\tilde{r}_{0i}$ in the metric space determined by $\mathcal{M}$,

$$\tilde{r}_{0i}^2 \equiv E_i = r_{0i}^T |\mathbf{H}|_{P_{i+1/2}} r_{0i}. \tag{17}$$

Hence, stencil points that generate a large interpolation error can be considered as distant points in the space induced by the metric $\mathcal{M}$, and we will use the length $\tilde{r}_{0i}$ in order to measure the distance between points P_0 and P_i in the 'data' space defined by the function $U(x, y)$. The new weight matrix $\tilde{\mathbf{W}}$ for the DWLS reconstruction is now written as

$$\tilde{W}_{ij} = \begin{cases} \tilde{r}_{0i}^{-p}, & i = j, \\ 0, & \text{otherwise};\ i, j = 1, 2, \ldots, N, \end{cases} \tag{18}$$

where we choose the polynomial degree $p = 2$. The brief outline of the algorithm can be as follows:

1. Define a reconstruction stencil $S = \{P_i\}$, $i = 1, \ldots, N$, for a given point P_0.
2. Compute the Hessian matrix at the edge midpoint $P_{i+1/2}$, $i = 1, \ldots, N$.
3. Compute the distance $\tilde{r}^2_{0i}$, $i = 1, \ldots, N$, as defined by (17).
4. Compute the weight function (18) for each point P_i, $i = 1, \ldots, N$ and use it for the DWLS approximation at point P_0.

Let us note here that the main computational effort in the new algorithm is related to the computation of the Hessian matrix at each edge midpoint in the reconstruction stencil. This is a task that requires further investigation as in many computational problems the Hessian is not readily available and estimates of second derivatives should be obtained in order to use the algorithm above. However, for the sake of discussion in the present paper we assume that the Hessian matrix is available in the problem.

Below we illustrate our approach by several numerical test cases. Our first test case is given by the isotropic function (6) considered in the previous section. It can be easily seen that the Hessian matrix $|\mathbf{H}|$ for function (6) is given the identity matrix $\mathbf{I}$. Hence, the weighting (18) in the solution space is equivalent to the weighting in the physical space, $\tilde{r}^2_{0i} = r^2_{0i}$. The geometrically distant point P_5 in the reconstruction stencil (7) is also a numerically distant point that should be eliminated by means of weighting (5).

The situation becomes quite different when the anisotropic function (11) is considered. Let us apply the new weight function (18) to the points P_1 through P_6 of the reconstruction stencil (12). The Hessian at each edge midpoint $P_{i+1/2}$, $i = 1, \ldots, 6$ of the stencil (12) is computed as

$$|\mathbf{H}| = \begin{bmatrix} 4 & 0 \\ 0 & 4B^2 e^{2By_{i+1/2}} \end{bmatrix}, \tag{19}$$

and the weight of point P_i in the data space is

$$\tilde{r}^2_{0i} = 4x_i^2 + 4B^2 e^{2By_{i+1/2}} y_i^2. \tag{20}$$

The results of the weighted reconstruction are $e(P_0) = 2.49141$ and $e_\nabla(P_0) =$ 3.05147e–01, so that we have a significant improvement in both the function error and the gradient error in comparison with the original result of $e(P_0) = 21.0549$ and $e_\nabla(P_0) = 65.0566$.

Let us imitate the grid refinement procedure for the reconstruction stencil (12) by halving the radius R of the circle C_R where the stencil points are located. The convergence rate for the unweighted and weighted approximation is presented in Fig. 3, where the function error (9) and the gradient error (10) are shown on a logarithmic scale in Figs. 3a and b, respectively. The error for the unweighted reconstruction is shown as a dashed line in the figure, while the error for the reconstruction that employs the weight function (18) is shown as a solid line. It can be seen from the figure that the convergence rate remains the same when we implement the data based weight function in the problem, as the function (11) is approximated by a linear polynomial in both cases. However, for any given radius R (where R can be thought of as the grid step size) the error of the weighted reconstruction is much smaller than the one computed for the unweighted reconstruction. The implementation of data dependent weights in the problem allows one to obtain accurate function approximation as well as to resolve the function gradient on a given coarse mesh.

The eigenvectors $\mathbf{r}_1$ and $\mathbf{r}_2$ defined by matrix $\mathbf{R}$ yield principal stretching directions in the Hessian-based metric space, the magnitudes of stretching in each direction being given by the Hessian eigenvalues $\lambda_1^{-1/2}$ and $\lambda_2^{-1/2}$. While in the previous test cases the Hessian was a diagonal matrix, our next test case is to consider the function where the stretching directions do not coincide with the canonical basis. Namely, we consider the Rosenbrock function,

$$U(x, y) = 100(y - x^2)^2 + (1 - x)^2, \tag{21}$$

where the points of the reconstruction stencil are again located along a circle of a given radius R as follows (see Fig. 2c),

$$P_i = (R \cos \gamma_i, R \sin \gamma_i), \tag{22}$$

$\gamma_i = \frac{\pi}{4}(2i - 1),\ i = 1, \ldots, 6$. The computation of the Hessian matrix results in the following weights in the data space

$$\tilde{r}_{0i}^2 = 1200 x_{i+1/2}^2 x_i^2 + 400 y_{i+1/2} x_i^2 - 800 x_{i+1/2} x_i y_i + 2x_i^2 + 200 y_i^2. \tag{23}$$

The convergence graphs for the unweighted and weighted DWLS reconstruction are shown in Fig. 4, where the notation in the figure is the same as in Fig. 3. It can be seen from the figure that the convergence rate for weighted approximation is the same as the convergence rate for the unweighted one. However, let us emphasize it again, that weighting of stencil points in the data space reduces the function error and the gradient error on 'coarse meshes' where the radius R is large enough. This result is very important for practical applications as it allows one to use DWLS reconstruction in a solution mesh adaptation procedure without losing the accuracy on coarse meshes.

Finally, let us consider a simple example of DWLS reconstruction in computational aerodynamics. Namely, the geometry shown in Fig. 5 presents a stencil on a stretched grid generated about an airfoil. Let stencil points P_i, $i = 1, \ldots, 4$, be defined as $P_1 = (-H, h_0)$, $P_2 = (0, h_1)$, $P_3 = (H, h_0)$ and $P_4 = (0, -h_2)$, where h_0, h_1, h_2 and H are grid parameters with $H \gg 1$, $H \gg h_0$, $h_0 \gg h_1$, $h_1 \gg h_2$. The parameter H is considered as a controlling parameter in the problem, so that the geometry in Fig. 5 is parametrized as $h_0 = \gamma_0 H$, $h_1 = \gamma_1 H$, $h_2 = \gamma_2 H$, positive constants $\gamma_2 \ll \gamma_0$, $\gamma_1 \ll \gamma_0$, $\gamma_0 \ll 1$ being fixed for given H. Let us note that points P_1, P_2 and P_3 can be thought of as points belonging to the airfoil boundary, and the choice of stencil points is explained by the requirement of generation of a high cell aspect ratio grid about an airfoil.

The function

$$U(x, y) = ax^2 + y, \tag{24}$$

is used to simulate the velocity gradient near the airfoil surface. The standard DWLS validation test case is to find the gradient of the function (24) by linear DWLS reconstruction at the origin $P_0 = (0, 0)$, where the exact gradient is $\nabla U(P_0) = (0, 1)$.

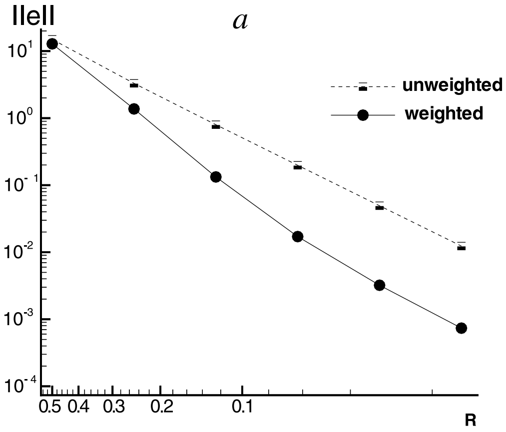

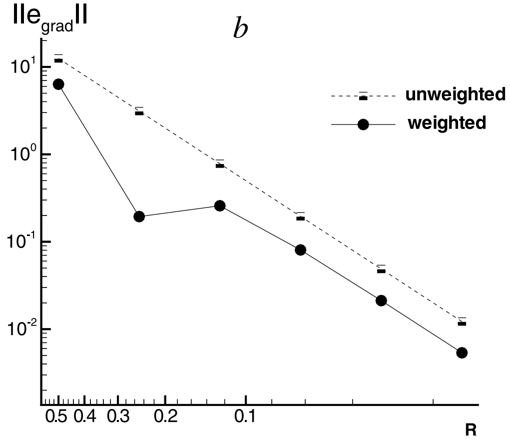

Fig. 4 The convergence rate for linear DWLS approximation of the function (21). The weight function (18) is used to eliminate numerically distant points from the stencil. (**a**) The function error (9) for the weighted (*solid line*) and unweighted (*dashed line*) approximation. (**b**) The gradient error (10) for the weighted (*solid line*) and unweighted (*dashed line*) approximation

Let $H = 100$, $\gamma_0 = 0.1$, $\gamma_1 = 0.01$, $\gamma_2 = 0.001$. We emphasize again that the values of H and γ_i, $i = 0, 1, 2$ reflect the point distribution at the curvilinear boundary that appears in real-life computations in the near field, and parameters γ_i cannot be increased for given H to make the stencil less stretched in the x-direction. Consider $a = -0.001$, then the gradient error (10) for the unweighted DWLS reconstruction (8) is $e_\nabla = 1.04022$. It has been originally concluded that the accuracy of the gradient reconstruction is poor because points P_1 and P_3 are geometrically distant points in the stencil and those points should be eliminated by means of weighting. Implementation of the weight function (5) with $p = 2$ in the problem gives us $e_\nabla = 1.64002\text{e–}02$, so that the gradient error is getting smaller when stencil points are weighted in the physical space.

Meanwhile, let us implement data dependent weights in the problem. The function (24) is a truly anisotropic function, as the matrix $|\mathbf{H}|$

$$|\mathbf{H}| = \begin{bmatrix} 2|a| & 0 \\ 0 & 0 \end{bmatrix}, \tag{25}$$

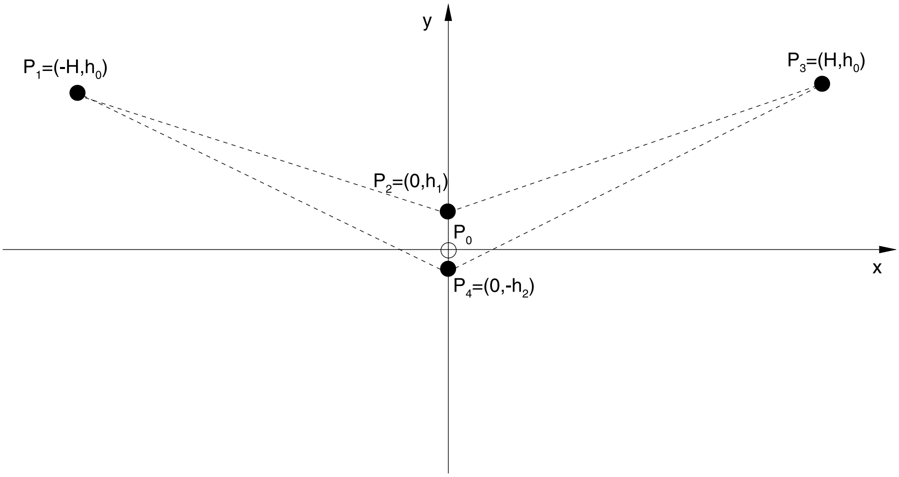

Fig. 5 The reconstruction stencil on an anisotropic mesh about an airfoil

has only one eigenvalue. The weights in the data space are then given by

$$\tilde{r}_{0i}^2 = 2|a|x_i^2, \tag{26}$$

and, unlike the weights in the physical space, they do not depend on the y-coordinate. The result of the weighting (26) in the data space is $e_\nabla = 9.53674\text{e–}10$, which is the gradient reconstruction with much better accuracy than that obtained by weighting in the physical space. Obviously, more test cases are required for numerical validation of data dependent weights but the first results obtained in the paper indicate that the weighting in the data space can be a promising technique for the gradient reconstruction in finite volume schemes on anisotropic meshes.

5 Concluding remarks

In our paper we have considered the problem of local approximation by a discontinuous weighted least-squares method when an irregular local support is used for the approximation. The need to study DWLS approximation with anisotropic support comes from computational applications (mainly from computational aerodynamics problems) where the method is widely used on irregular unstructured meshes. The support set on such meshes contains distant points that make a negative impact on the accuracy of the DWLS reconstruction. While the inverse distance weight function has been well investigated by many authors for points that are remote in the physical space, it has been discussed in the paper that another type of distant points may appear in the reconstruction stencil. Those points (called numerically distant points in the paper) appear in reconstruction stencil as a result of poor function resolution on irregular coarse meshes. The numerically distant points affect the accuracy of the DWLS reconstruction but they cannot be eliminated from the stencil by inverse distance weighting.

It has been suggested in the paper that the numerically distant points have to be weighted in the data space in order to remove them from a DWLS reconstruction stencil. Thus we have designed a new approach that allows one to measure distance between points in the data space. Implementation of data dependent weights in order to suppress numerically distant points in the stencil resulted in much better accuracy in test cases considered in the paper. The results obtained in the paper are also important for MSL approximation as they may help one to better understand what support set would be optimal for a given function.

While it has been shown in the paper that weighting in the data space presents an efficient alternative to weighting in the physical space, several questions remain that require further thorough discussion and should become a focus of future work. The most important issue is to validate an error estimate used to design weight coefficients in the data space. Also, as we have already mentioned it in the paper, it is often that the Hessian matrix is not available in practical applications where DWLS approximation is required. Thus a reliable estimate of the matrix of second derivatives should be obtained. Once the above-mentioned questions have been sorted out, the extension of the method to the 3-D case becomes a straightforward task that should not be computationally expensive as weighted DWLS reconstruction still uses a local reconstruction stencil. However, the computational cost of the algorithm should be further investigated and that is considered as another topic of future work.

References

1. Alexa, M., Behr, J., Cohen-Or, D., Fleishman, S., Levin, D., Silva, T.C.: Computing and rendering point set surfaces. IEEE Trans. Vis. Comput. Graph. **9**(1), 3–15 (2003)
2. Atluri, S.N., Kim, H.-G., Cho, J.Y.: A critical assessment of the truly meshless local Petrov-Galerkin (MLPG) and Local Boundary Integral Equation (LBIE) methods. Comput. Mech. **24**, 348–372 (1999)
3. Barth, T.J.: A three-dimensional upwind Euler solver for unstructured meshes. AIAA 91-1548 (1991)
4. Barth, T.J., Jespersen, D.C.: The design and application of upwind schemes on unstructured meshes. AIAA 89-0366 (1989)
5. Bates, D.M., Watts, D.G.: Nonlinear Regression Analysis and Its Applications. Wiley, New York (1988)
6. Bjőrck, A.: Numerical Methods for Least-Squares Problems. SIAM, Philadelphia (1996)
7. Breitkopf, P., Naceur, H., Rassineux, A., Villon, P.: Moving least squares response surface approximation: Formulation and metal forming applications methods. Comput. Struct. **83**, 1411–1428 (2005)
8. d'Azevedo, E.F., Simpson, R.B.: On optimal interpolation triangle incidences. SIAM J. Sci. Stat. Comput. **10**, 1063–1075 (1989)
9. Lancaster, P., Salkauskas, K.: Surfaces generated by moving least squares methods. Math. Comput. **37**(155), 141–158 (1981)
10. Mavriplis, D.J.: Revisiting the least-square procedure for gradient reconstruction on unstructured meshes. AIAA 2003-3986 (2003)
11. Most, T., Bucher, C.: New concepts for moving least squares: An interpolating non-singular weighting function and weighted nodal least squares. Eng. Anal. Bound. Elem. **32**, 461–470 (2008)
12. Neter, J., Wasserman, W., Kutner, M.H.: Applied Linear Statistical Models. Richard D. Irwin (1985)
13. Nie, Y.F., Atluri, S.N., Zou, C.W.: The optimal radius of the support of radial weights used in moving least squares approximation. CMES: Comput. Model. Eng. Sci. **12**(2), 137–147 (2006)
14. Peraire, J., Vahdati, M., Morgan, K., Zienkiewicz, O.C.: Adaptive remeshing for compressible flow computations. J. Comput. Phys. **72**, 449–466 (1987)
15. Perko, J., Šarler, B.: Weight function shape parameter optimization in meshless methods for non-uniform grids. CMES: Comput. Model. Eng. Sci. **19**(1), 55–68 (2007)
16. Petrovskaya, N.B.: Discontinuous weighted least-squares approximation on irregular grids. CMES: Comput. Model. Eng. Sci. **32**(2), 69–84 (2008)

17. Petrovskaya, N.B.: Quadratic least-squares solution reconstruction in a boundary layer region. Commun. Numer. Methods Eng. doi:10.1002/cnm.1259
18. Prax, C., Salagnac, P., Sadat, H.: Diffuse approximation and control-volume-based finite-element methods: A comparative study. Numer. Heat Transf. B **34**, 303–321 (1998)
19. Press, W.H., Flannery, B.P., Teukolsky, S.A., Vetterling, W.T.: Numerical Recipes in Fortran 77: The Art of Scientific Computing. Cambridge University Press, Cambridge (1996) .
20. Smith, T., Barone, M., Bond, R., Lorber, A., Baur, D.: Comparison of reconstruction techniques for unstructured mesh vertex centered finite volume schemes. AIAA 2007-3958 (2007)
21. Stoer, J.R., Bulirsch, R.: Introduction to Numerical Analysis. Springer, New York (1980)
22. Thomas, J.L., Diskin, B.: Towards verification of unstructured-grid solvers. AIAA-2008-666 (2008)
23. Wendland, H.: Piecewise polynomial, positive definite and compactly supported radial basis functions of minimal degree. Adv. Comput. Math. **4**, 389–396 (1995)